Relativistic flows and particle acceleration

J. G. Kirk john.kirk@mpi-hd.mpg.de

Max-Planck-Institut für Kernphysik, Postfach 10 39 80, 69029 Heidelberg, Germany

Summary. Relativistic bulk motion is known to occur in several astrophysical contexts. In each case, nonthermal radiation from relativistic electrons is detected, requiring the acceleration of electrons to high energy in the local plasma frame. This situation has motivated the generalisation of the theory of diffusive particle acceleration to apply to the case of mildly relativistic flows, and, more recently, to flows of arbitrary Lorentz factor. The kinematic theory of particle acceleration at ultrarelativistic shocks leads to the prediction of a high-energy spectral index of -1.1 for the energy flux of synchrotron photons. However, several effects can change this picture. This paper summarises the basic theory and discusses some recent extensions. Application of the theory to the spectrum of the Crab Nebula suggests an additional acceleration mechanism is responsible for low energy electrons.

1 Introduction

In nonrelativistic flows, the first order Fermi process operating at a shock front has been applied in a wide variety of astrophysical situations and has been the subject of considerable theoretical effort — with interest currently focused on nonlinear aspects [1]. Fundamentally, this mechanism relies on the isotropisation of energetic charged particles in the vicinity of the shock front by magnetic fluctuations, which may be self-generated. In relativistic flows, magnetic fluctuations can also be expected to scatter energetic particles. However, simple kinematics dictates that the distribution function cannot be isotropised at the shock front. Seen from the upstream plasma, those particles which run ahead of a relativistic shock occupy a small cone in velocity space centred around the velocity of the shock. A small deflection quickly results in the particle being recaptured by the shock front. Consequently, in the absence of large-angle scattering events, most of velocity space remains unpopulated. Seen from the downstream frame, this translates into a hole in the angular distribution centred around the velocity of the upstream plasma. Under these conditions, the diffusion approximation cannot be applied close to the shock front; a different approach is needed, which is able to account for the intrinsic anisotropy of the particle distribution functions [2].

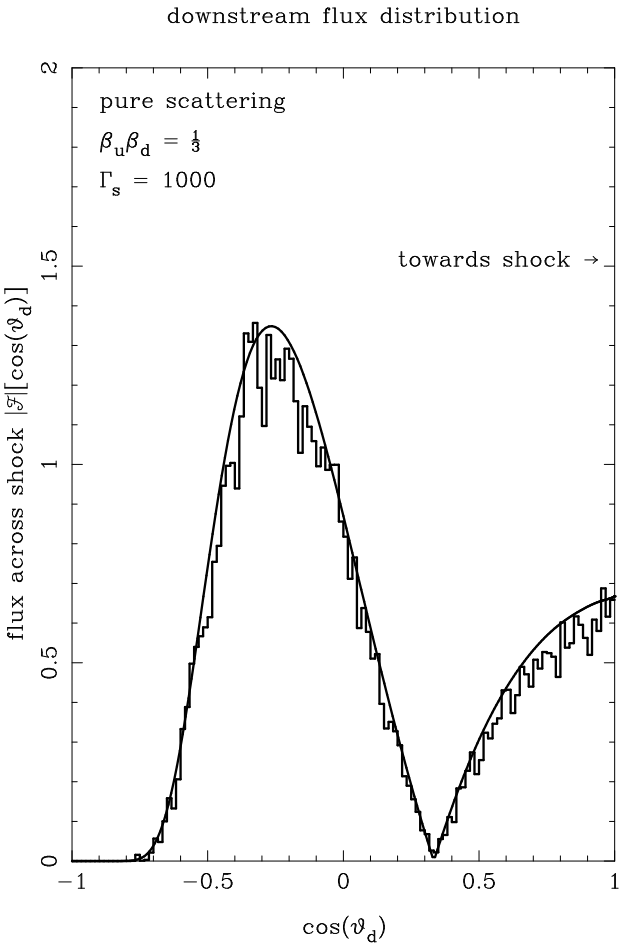

Fig. 1. A comparison (from [5]) between a Monte-Carlo simulation and the analytic result for the particle flux across a shock front as a function of the cosine of the angle $\theta_{\rm d}$ between the particle velocity and the shock normal measured in the frame in which the downstream plasma is at rest. $\theta_{\rm d} = 0$ corresponds to motion along the normal from downstream to upstream. Jump conditions for a relativistic gas are used and the upstream plasma has a Lorentz factor $\Gamma = 1000$.

2 Kinematics

The *kinematic* problem of particle acceleration at a relativistic shock, i.e., that of finding the distribution of a collection of test particles undergoing small-angle, random, elastic (in the plasma frame) deflections in the vicinity of a discontinuity in the (relativistic) plasma velocity is well-understood. An analytic method based on an eigenvalue decomposition is available which gives the spectrum and angular dependence of the distribution function at energies well above those of injection for

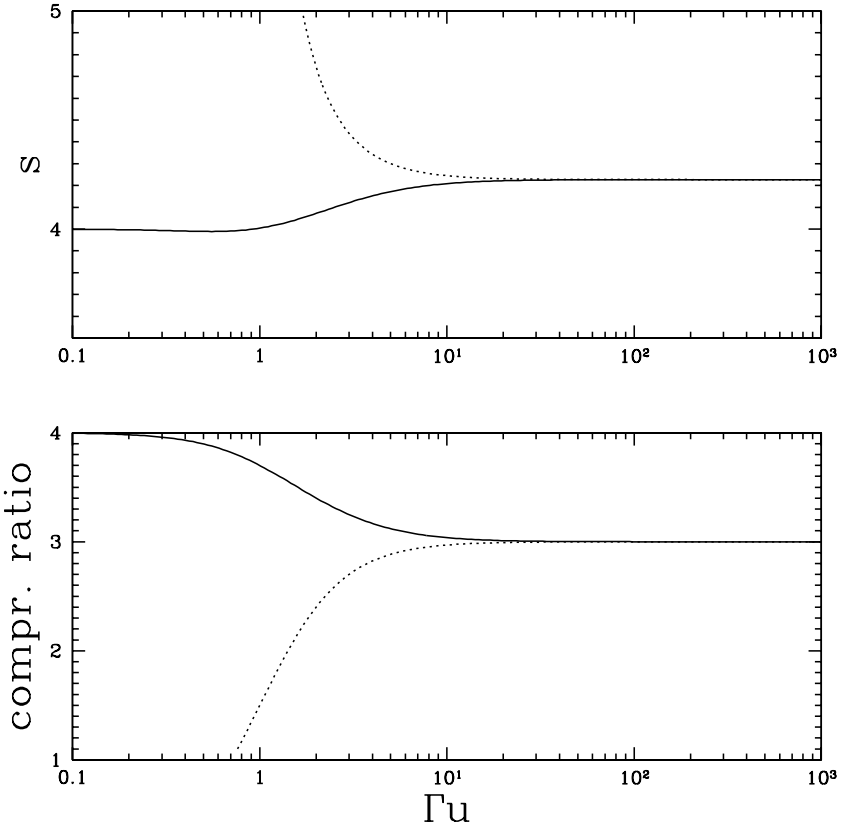

Fig. 2. The high-energy power-law index s (upper panel) and compression ratio (lower panel) as a function of the spatial component of the upstream four speed Γu. The dotted line refers to a shock in a gas with negligible rest-mass and the solid line to a strong shock (i.e., cold upstream medium) in an ideal gas with adiabatic index 5/3.

arbitrary shock speeds [3]. In addition, Monte-Carlo simulations have been performed, finding results which are in good agreement with the analytic approach [4, 5]. These results are illustrated in Figs. 1 and 2.

Well above the injection energy the phase-space density f is a power-law in momentum: $f \propto p^{-s}$ and at the shock front the angular dependence is well-approximated by the simple expression

$$f \propto (1-\mu_{\rm s}u)^{-s} \exp\left(-\frac{1+\mu_{\rm s}}{1-\mu_{\rm s}u}\right) \tag{1}$$

where $\mu_{\rm s}$ is the cosine of the angle between the shock normal and the particle velocity $c\boldsymbol{u}$ measured in the frame in which the shock is at rest and the upstream plasma

flows along the shock normal. This expression displays the expected hole in the angular distribution: $f \to \left(2\Gamma^2\right)^s \exp\left(-2\Gamma^2\right)$ for $\mu_{\rm s} = 1$. In Fig. 1, which shows the particle flux $\mu \times f$ in the downstream reference frame, this is seen at $\cos(\theta_{\rm d}) = -1$.

Fig. 2 shows the compression ratio and the high-energy power-law index s as a function of the spatial component of the 4-speed Γu of the upstream plasma, where $\Gamma = (1-u^2)^{-1/2}$. An interesting aspect of these results is that the power-law index tends asymptotically to the value $s \approx 4.23$ for large shock Lorentz factors (or, equivalently, upstream Lorentz factors), independent of the equation of state of the plasma. This asymptotic value is essentially fixed by the compression ratio of the shock and depends only weakly on the form of the scattering operator used to describe the small-angle deflections [3].

An isotropic small-angle scattering operator was used to compute the results shown in Figs. 1 and 2. This causes the particle's velocity vector to diffuse around on a sphere in a manner independent of its direction. Since shock crossings are the only events of relevance for acceleration, the transport equation contains only the angle between the velocity and the shock normal. In this case, the direction of the average magnetic field plays no role.

There is an important difference between this operator and the scattering operator conventionally used in nonrelativistic theory. The nonrelativistic picture assumes it is reasonable to define the trajectory of a particle between scatterings (the unperturbed motion) in terms of the motion of its guiding centre. Scatterings cause a change in the pitch-angle, leading to the diffusion of particles along magnetic field lines. Cross-field diffusion, on the other hand, is usually neglected in this picture (e.g., [6]). However, as seen in the frame of the downstream medium, the magnetic field carried towards a shock by an upstream plasma flowing at high Lorentz factor appears to lie almost in the plane of the shock front. As a consequence, highly relativistic shocks are *perpendicular* shocks [7] which cannot be multiply crossed by particles diffusing along field lines. Cross-field transport is essential to the operation of the first-order Fermi mechanism in this configuration.

In a uniform field, a particle which crosses a relativistic shock front from downstream to upstream will be recaptured by the front after executing a small fraction of roughly $\sim 1/\Gamma$ of a gyration, as illustrated qualitatively in Fig. 3. Thus, if scattering plays a role, it is reasonable to describe the unperturbed trajectory not as a helix, but as a straight line. This is especially true if, as expected (see next section), the field is highly nonuniform on the length scale of a gyro radius. In this case the role of the average field (if it exists) ceases to be important, and the description of the stochastic trajectory is in terms of deflections of the velocity, rather than changes in pitch angle. This is the form of operator used in the analytic approach. In Monte-Carlo treatments, on the other hand, it is possible to retain the effect of an average field [8, 5] but little difference is found, provided the turbulence remains strong. However, as expected, the acceleration mechanism becomes less effective as the turbulence diminishes [9]. Explicit calculations of particle motion in a random magnetic field have also been performed [10, 11] and used to compute the acceleration around a relativistic shock for Lorentz factors $\Gamma \leq 5$ [10] and, more recently, for $\Gamma \leq 100$ [12]. The latter find good agreement with the analytic result on the asymptotic power-law index.

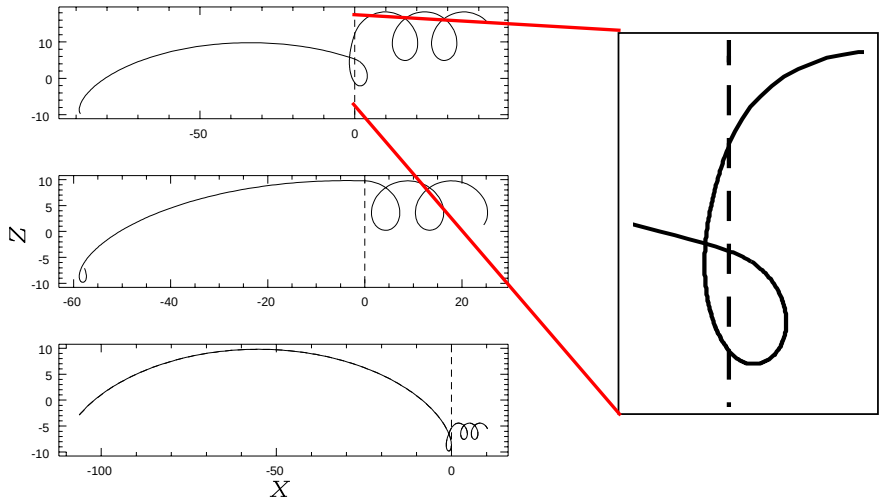

Fig. 3. Unperturbed (scatter-free) particle trajectories at a relativistic shock (located at $x = 0$), seen in the shock rest frame. The magnetic field is in the y direction and an electric field in the z direction causes particles to drift into and out of the shock with the plasma bulk speed. Depending on the initial phase, particles from upstream ($x < 0$) cross the shock one or more times, during which their gyrocentre shifts in z, causing an increase or decrease in the particle energy. The inset illustrates that a particle performs only a small fraction of a gyration upstream before being recaptured by the shock, even in this mildly relativistic example ($\Gamma = 5$).

3 Nonlinear effects and magnetic field generation

In contrast with the situation in nonrelativistic shocks [1], the nonlinear modification of relativistic shock does not affect the asymptotic power-law index at high particle energy, provided the scattering mean-free path of these particles increases with energy (as is to be expected for scattering off magnetic fluctuations). There are two reasons for this: firstly, isotropised, accelerated particles behave like a relativistic gas with adiabatic index 4/3, so that the overall compression ratio of an ultra-relativistic shock front remains unchanged, even when a significant part of the overall energy and momentum flux is carried by these particles. Secondly, the asymptotic power-law index in the test-particle picture is *soft* (i.e., $s > 4$). This means that it is possible to consider a Lorentz factor above which the test-particle approximation is valid, because the energy density in the remaining accelerated particles is indeed small. Nevertheless, a strong nonlinear effect can be exerted by particles of lower energies, whose mean free path to scattering is comparable to the size of internal structures in the shock transition [13].

The most promising mechanism of formation of relativistic shock in a collisionless plasma involves the nonlinear evolution of the Weibel instability [14, 15, 16], which generates magnetic field perpendicular to the relative streaming motion of the up and downstream plasmas i.e., in the plane of the incipient shock. A full simulation of this situation has not yet been performed, but recent 3D-PIC simulations of colliding

plasma shells [17, 18, 19] suggest that a downstream magnetic field can be generated with a strength up to $\sigma \approx 1\%$. (Here the magnetisation parameter σ is defined as the ratio of the magnetic energy density to twice the total enthalpy density (including rest mass) as measured in the plasma rest frame). This is encouraging, since it is roughly the level implied by spectral modelling [20] of GRB after-glows.

The spectrum of accelerated particles is certainly closely tied to the evolution of the turbulent magnetic field. However, if we are interested only in high energy particles of long mean free path, the power-law index predicted by the first-order Fermi mechanism can be calculated simply by modifying the shock jump conditions to account for the generated field as a large amplitude wave in the downstream plasma. In a time averaged picture, linear functions of the wave fields vanish and the stress-energy tensor in the plasma frame is

$$T^{\mu\nu} = \left(w + \frac{B^2}{4\pi}\right) u^\mu u^\nu + \left(p + \frac{B^2}{8\pi}\right) g^{\mu\nu} - \frac{B^\mu B^\nu}{4\pi} \tag{2}$$

(for notation see [2]). The last term on the right hand side does not contribute to the fluxes across the shock front if the generated magnetic field lies in the shock plane. As a result, the jump conditions are the same as those of an unmagnetised fluid, provided the magnetic enthalpy density $B^2/4\pi$ and pressure $B^2/8\pi$ are taken into account [21]. For a relativistic gas, this gives an effective adiabatic index

$$\gamma_{\rm eff} = \frac{4(1+\sigma)}{(3+\sigma)} \tag{3}$$

leading to an asymptotic compression ratio of $1/\left(\gamma_{\rm eff} - 1\right)$ and a relative speed of the upstream medium with respect to the downstream medium corresponding to a Lorentz factor $\Gamma_{\rm rel} = \Gamma\sqrt{(2-\gamma_{\rm eff})/\gamma_{\rm eff}}$ (where Γ is the Lorentz factor of the shock front seen in the upstream medium). As σ increases, the compression ratio of the shock decreases and the high-energy power-law softens, as shown in Fig. 4.

4 Application to the Crab Nebula

A relativistic wind carries energy from the Crab pulsar out to the Nebula. This energy is released into nonthermal particles at a termination shock, which is probably the best observed example of a relativistic shock in the universe. The average Lorentz factor of the upstream plasma can be estimated from the spin-down luminosity of the pulsar and the total number of electrons and positrons which have accumulated in the Nebula [22] to be between $\sim 10^4$ and 10^6. This is well into the asymptotic region of high Γ as far as the first-order Fermi process is concerned, and the X-ray synchrotron emission [23] indeed exhibits a power-law index of $s = 4.2$, as predicted for a plasma in which the magnetic energy plays no dynamical role [24].

However, the integrated synchrotron spectrum displays not only the expected "cooling break" at a frequency where the characteristic cooling time corresponds roughly to the age of the object, but also a second break at higher frequency [24]. This is presumably due to an intrinsic feature of the acceleration process and probably characterises the transition between two different mechanisms. One possibility is that the break energy reflects the different spatial scales associated with ions and electrons/positrons. Regarded as distinct fluids, these components would be

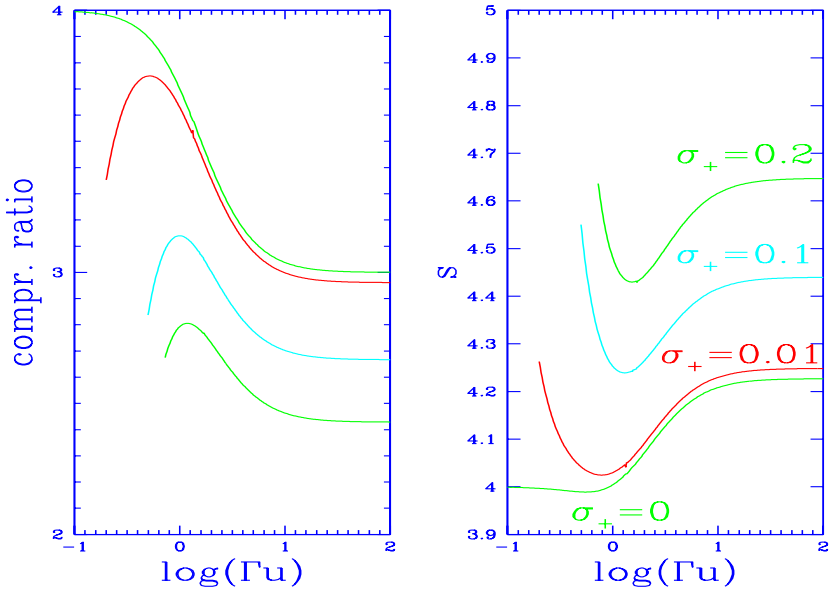

Fig. 4. The compression ratio and power-law index s for a gas of adiabatic index 5/3 in which a magnetic field is generated downstream to the level $\sigma = \sigma_+$ (see text for notation).

expected to produce shock structures each on the scale of the thermal gyro radius: $\Gamma Mc^2/eB$ and $\Gamma mc^2/eB$, respectively. However, strong heating of the electron/positron gas, perhaps via the maser mechanism proposed by Hoshino et al [25], should result in a smearing out of the smaller of these two scales. Below Lorentz factors of roughly $\Gamma M/m$, the hard ($s \approx 3$) maser mechanism should dominate over the first-order mechanism for electrons and positrons. An alternative explanation, which assumes the ions in the Crab wind carry very little of the energy flux, is that magnetic field dissipation within the shock front is responsible [21].

Although it is at present not known which (if any) of these theories is correct, the implications for modelling the spectra of sources which display relativistic bulk motion are clear: nonthermal electrons are likely to be injected with an intrinsic spectrum exhibiting a break. Hard spectra ($s < 4$) that concentrate energy at the highest Lorentz factors arise in connection with maser mechanisms and with reconnection [26], but are not predicted from the first-order Fermi mechanism at a relativistic shock. The signature of the latter, which should emerge at higher electron energy, is a soft spectrum with a power law index of the phase space distribution ranging from 4.2 to about 4.4, depending on the efficiency of magnetic field generation.

References

1. M. Malkov, L.O'C. Drury: Rep. Prog. Phys. **64**, 429 (2001)

2. J.G. Kirk, P. Duffy: J. Phys. G: Nucl. Part. Phys. **25**, R163 (1999)
3. J.G. Kirk, A.W. Guthmann, Y.A. Gallant, A. Achterberg: ApJ **542**, 235 (2000)
4. J. Bednarz, M. Ostrowski: Phys. Rev. Letts. **80**, 3911 (1998)
5. A. Achterberg, Y.A. Gallant, J.G. Kirk, A.W. Guthmann: MNRAS **328**, 393 (2001)
6. J.G. Kirk, A.F. Heavens: MNRAS **239**, 995 (1989)
7. M.C. Begelman, J.G. Kirk: ApJ **353**, 66 (1990)
8. M. Ostrowski: 1983 MNRAS **264**, 248 (1993)
9. M. Ostrowski, J. Bednarz: A&A **394**, 1141 (2002)
10. K.R. Ballard, A.F. Heavens: MNRAS **259**, 89 (1992)
11. F. Casse, M. Lemoine, G. Pelletier: Phys. Rev. D **65**, 023002 (2002)
12. M. Lemoine, G. Pelletier: ApJ **589**, L73 (2003)
13. D.C. Ellison, G.P. Double: Astroparticle Phys. **18**, 213 (2002)
14. T.Y.B. Yang, Y. Gallant, J. Arons, A.B. Langdon: Physics of Fluids B – Plasma Physics **5**, 3369 (1993)
15. T.Y.B. Yang, J. Arons, A.B. Langdon: Physics of Plasmas **1**, 3059 (1994)
16. M.V. Medvedev, A. Loeb: ApJ **526**, 679 (1999)
17. J. Sakai, T. Nakayama, Y. Kazimura, S. Bulanov: J. Phys. Soc. Japan **69**, 2503 (2000)
18. R.A. Fonseca, L.O. Silva, J.W. Tonge, W.B. Mori, J.M. Dawson: Physics of Plasmas **10**, 1979 (2003)
19. L.O. Silva, R.A. Fonseca, J.W. Tonge, J.M. Dawson, W.B. Mori, M.V. Medvedev: ApJ **596**, L121 (2003)
20. A. Panaitescu, P. Kumar: ApJ **571**, 779 (2002)
21. Y. Lyubarsky: MNRAS, **345**, 153 (2003)
22. J.G. Kirk, O. Skjæraasen: ApJ **591**, 366 (2003)
23. R. Willingale, B. Aschenbach, R.G. Griffiths, S. Sembay, R.S. Warwick, W. Becker, A.F. Abbey, J.M. Bonnet-Bidaud: A&A **365**, L212 (2001)
24. Y. Gallant, E. van der Swaluw, J.G. Kirk, A. Achterberg: Modelling plerion spectra and their evolution. In: *Neutron Stars in Supernova Remnants* ASP conference series **271**, eds: P.O. Slane, B.M. Gaensler p. 161
25. M. Hoshino, J. Arons, Y.A. Gallant, A.B. Langdon: ApJ **390**, 454 (1992)
26. S. Zenitani, M. Hoshino: ApJ **562**, L63 (2001)